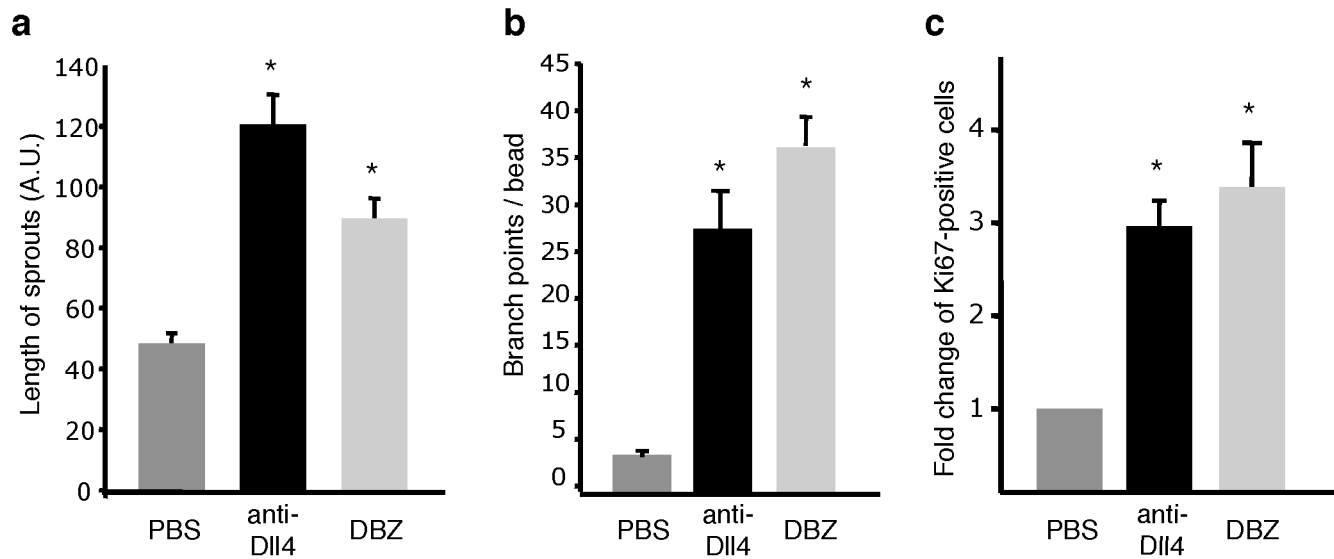
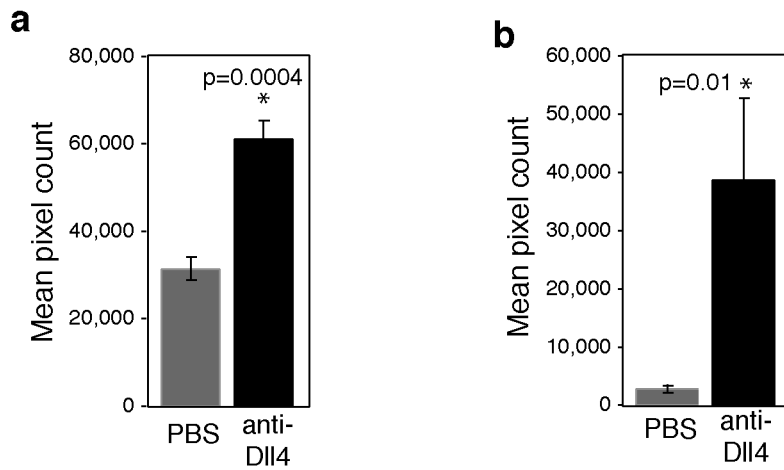


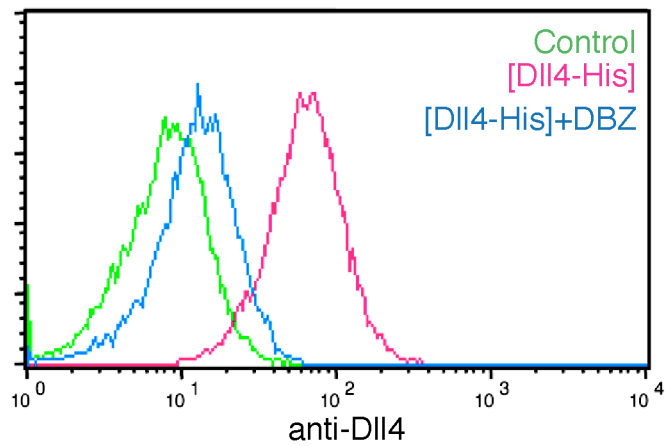
**Supplementary Figure 1 | Characterization of anti-DII4.** **a**, Epitope mapping of anti-DII4 (YW152F). Schematic representation of a set of DII4 mutants expressed as C-terminal human placental alkaline phosphatase (AP) fusion proteins. 293T cell conditioned media containing the fusion proteins were tested on 96-well microtiter plates coated with purified anti-DII4 (YW152F, 0.5  $\mu$ g/ml). The bound DII4.AP was detected using 1-Step PNPP (Pierce) as substrate and OD 405 nm absorbance measurement. **b-d**, Selective binding of YW152F to DII4. 96-well Nunc Maxisorp plates were coated with purified recombinant proteins as indicated (1  $\mu$ g/ml). The binding of YW152F at indicated concentrations was measured by ELISA assay. Bound antibodies were detected with anti-human antibody HRP conjugate using TMB as substrate and OD 450 nm absorbance measurement. Anti-HER2 and recombinant ErbB2-ECD were used as assay control (**b**). FACS analysis of 293 cells transiently transfected with vector, full length DII4, Jag1 or DII1. Significant binding of YW152F was only detected on DII4 transfected cells (top panel). Expression of Jag1 and DII1 was confirmed by the binding of recombinant rat Notch1-Fc (rrNotch1-Fc, middle panel) and recombinant rat Notch2-Fc (rrNotch2-Fc, bottom panel), respectively. YW152F, rrNotch1-Fc or rrNotch2-Fc (R& D system) was used at 2  $\mu$ g/ml, followed by goat anti-human IgG-PE (1:500, Jackson ImmunoResearch) (**c**). Anti-DII4 blocked the binding of DII4-AP, but not DII1-AP, to coated rNotch1, with a calculated  $IC_{50}$  of  $\sim$ 12 nM (left panel). Anti-DII4 blocked the binding of DII4-His, but not Jag1-His, to coated rNotch1, with a calculated  $IC_{50}$  of  $\sim$ 8 nM (right panel) (**d**). **e**, Specific binding of YW152F to endogenously expressed DII4. FACS analysis of HUVECs transfected with control or DII4-specific siRNA. YW152F was used at 2  $\mu$ g/ml, followed by goat anti-human IgG-PE (1:500, Jackson ImmunoResearch).



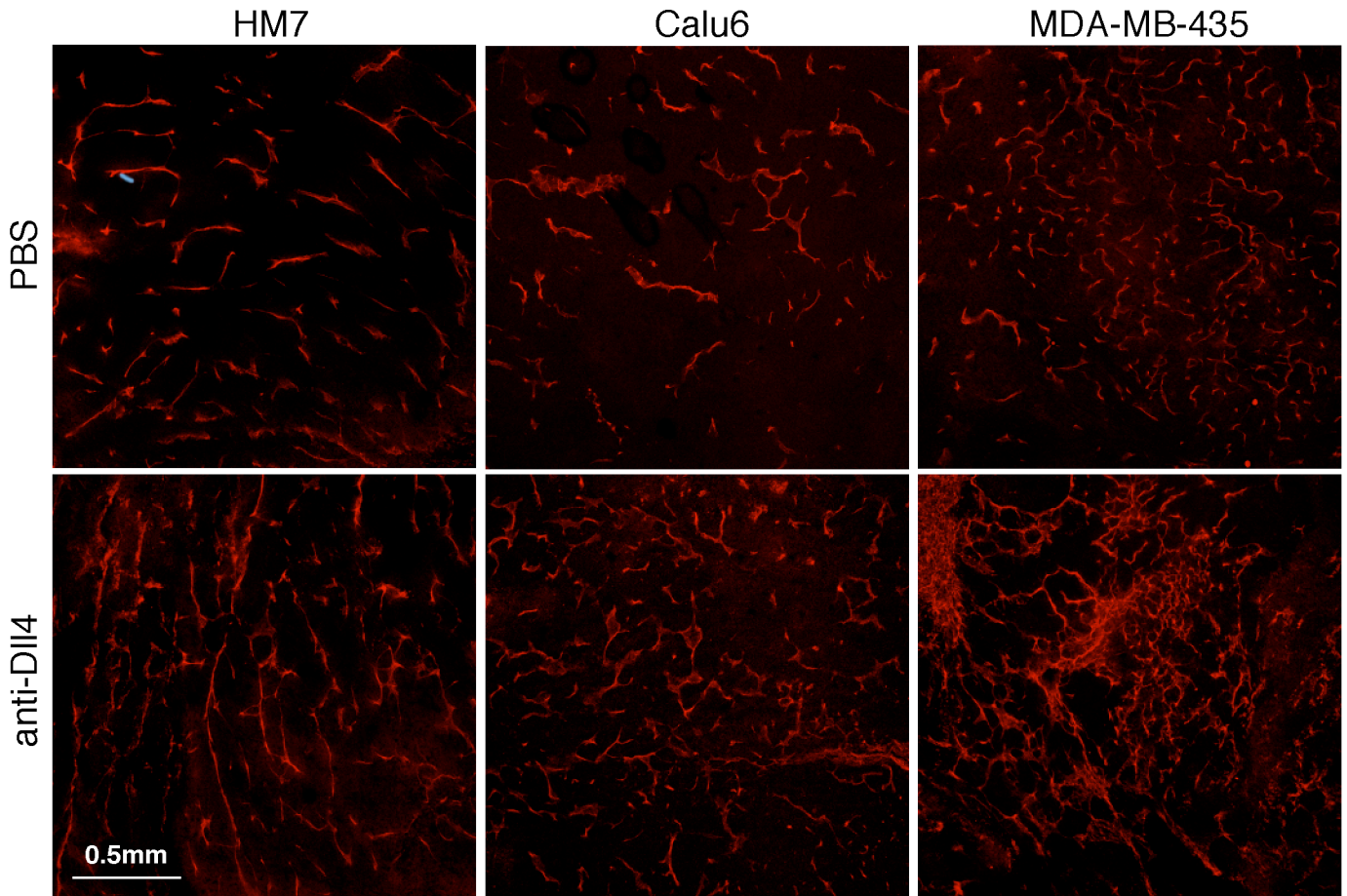
**Supplementary Figure 2 | Blocking DII4/Notch increases EC sprouting in 3-D fibrin gel.** HUVEC sprouting assays in 3-D fibrin gel in the presence of anti-DII4 (5  $\mu\text{g/ml}$ ) or DBZ (0.08  $\mu\text{M}$ ) for 7 days. Quantification of average sprout length (n=10 beads) (**a**). Quantification of branch points of sprouts (n=10 beads) (**b**). Quantification of Ki67-positive cells (n=10 beads) (**c**). Results are representative of 3-6 independent experiments. \* denotes  $P < 0.01$ . A.U., Arbitrary Units.



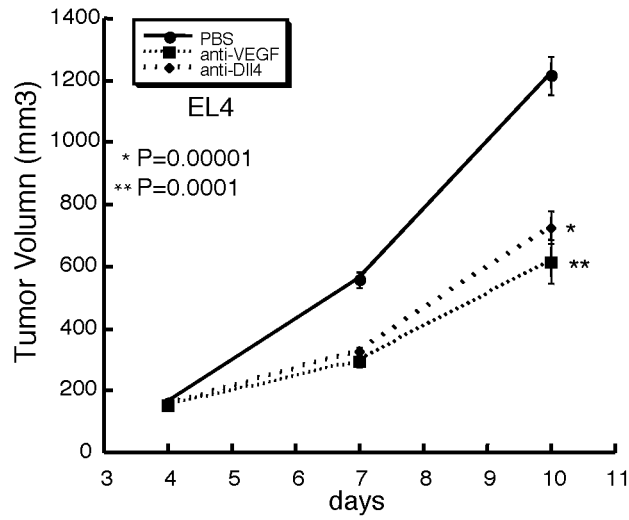
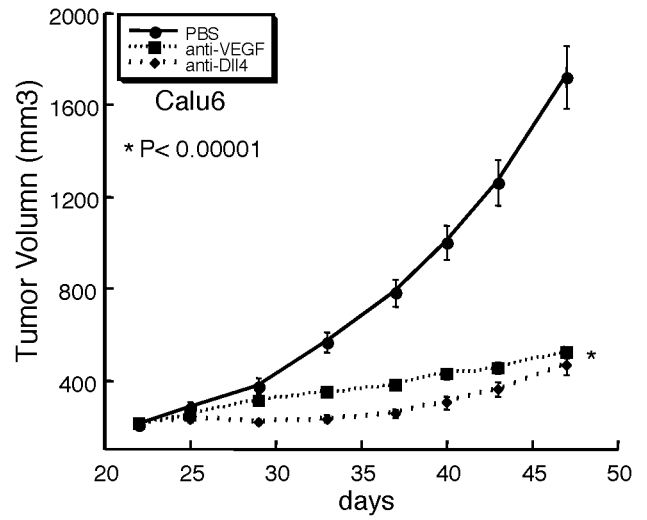
**Supplementary Figure 3 | Blocking Dll4/Notch by systemic delivery of anti-Dll4 results in accumulation of ECs in neonatal retinas.** Quantification of EC density (isolectin staining) in P5 retinas from PBS or anti-Dll4 treated mice (n= 8 images) **(a)**. Quantification of EC proliferation (Ki67 staining) in P5 retinas from PBS or anti-Dll4 treated mice (n= 8 images) **(b)**. Images of fluorescent staining were analyzed using NIH Image J. Bars represent mean pixel count  $\pm$  s.d. Results are representative of 3 independent experiments.



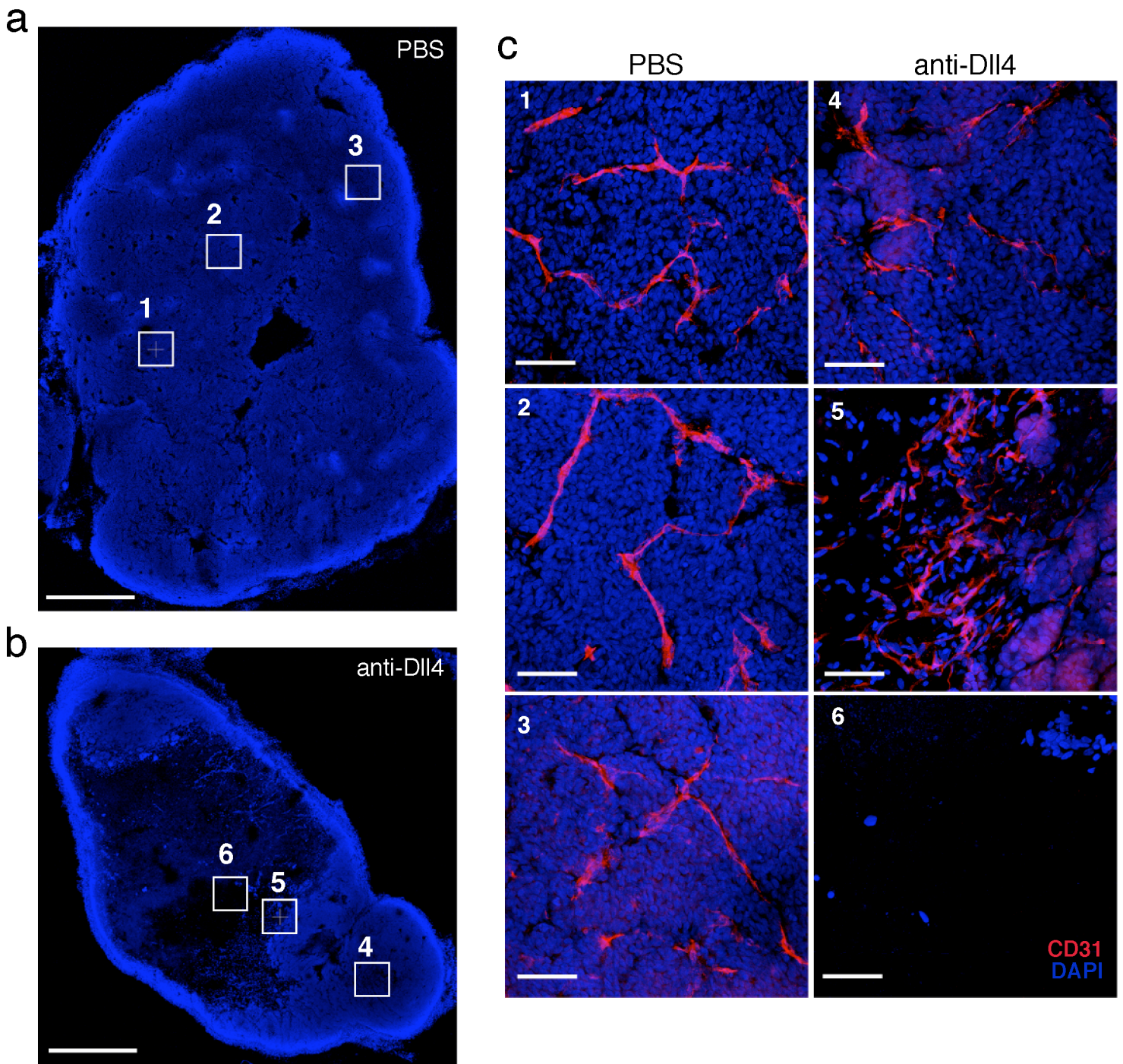
**Supplementary Figure 4 | Upregulation of DII4 by Notch activation.** HUVECs were stimulated by immobilized C-terminal His-tagged human DII4 (amino acids 1-404) in the absence or presence of DBZ (0.08  $\mu$ M). 36 hr after stimulation, expression of endogenous DII4 was examined by FACS analysis with anti-DII4.



**Supplementary Figure 5 | Blocking Dll4/Notch results in increase of EC density in tumors.** Immunohistochemistry of anti-CD31 in representative sections of HM7, Calu6 or MDA-MB-435 tumors from control or anti-Dll4 treated mice.

**a****b**

**Supplementary Figure 6 | Effect of anti-DII4 and anti-VEGF on tumor growth.** Mice bearing EL4 mouse tumors (**a**) or Calu6 human xenograft tumors (**b**) were treated with anti-DII4 or anti-VEGF (5 mg/kg, twice weekly). Mean tumor volumes with SEs are presented (n=10).



**Supplementary Figure 7 | Selective blocking of Dll4 results in poor vascular function in Colo205 xenograft tumor.** Tumor vascular histology studies of Colo205 tumors. Overviews of DAPI staining of representative tumor sections from PBS (**a**) or anti-Dll4 (**b**) treated mice. Anti-CD31 immunostainings of regions marked as 1-3 (**a**) and 4-6 (**b**) are shown in (**c**). Viable tumor cells are present in most regions of the PBS treated tumor as indicated by the relatively uniform and dense DAPI staining (**a**). In contrast, in anti-Dll4 treated tumor, the healthy tumor mass is greatly reduced as evidenced by the uneven and sparse DAPI staining (**b**). This becomes more pronounced in the central region of the tumor. In anti-Dll4 treated tumor, there are regions (for instance, region 5 in panel **c**) where high EC density (anti-CD31) is associated with low viable tumor content (low DAPI staining), suggesting that these ECs fail to form functional tumor vessels to support tumor growth and/or survival. Scale bars, 1 mm in (**a**) and (**b**), and 0.1 mm in (**c**), respectively.